Marine Geology xxx (xxxx) xxx–xxx

Contents lists available at ScienceDirect

Marine Geology

journal homepage: www.elsevier.com/locate/margo

Multiple dating approach (^{14}C, ^{230}Th/U and ^{36}Cl) of tsunami-transported reef-top boulders on Bonaire (Leeward Antilles) – Current achievements and challenges

Gilles Rixhon[a,*], Simon Matthias May[a], Max Engel[a], Silke Mechernich[b], Andrea Schroeder-Ritzrau[c], Norbert Frank[c], Jens Fohlmeister[c], Frédéric Boulvain[d], Tibor Dunai[b], Helmut Brückner[a]

[a] Institute of Geography, University of Cologne, Cologne, Germany
[b] Institute of Geology and Mineralogy, University of Cologne, Cologne, Germany
[c] Institute of Environmental Physics, University of Heidelberg, Germany
[d] Department of Geology, University of Liège, Belgium

ARTICLE INFO

Keywords:
Reef-top boulders
Tsunami transport
^{14}C dating
^{230}Th/U dating
^{36}Cl surface exposure dating
Bonaire

ABSTRACT

Dating the transport/deposition time of supratidal coarse-clast deposits is difficult, limiting their value for inferring frequency-magnitude patterns of high-energy wave events. On Bonaire (Leeward Antilles, Caribbean), these deposits form prominent landforms, and transport by one or several Holocene tsunamis is assumed at least for the largest clasts. Although a large dataset of ^{14}C and electron spin resonance (ESR) ages is available for major coral rubble ridges and ramparts, it is still debated whether these data reflect the timing of major events, and how these datasets are biased by the reworking of coral fragments. As an attempt to overcome the current challenges for dating the dislocation of singular boulders, three distinct dating methods are implemented and compared: (i) ^{14}C dating of boring bivalves attached to the boulders; (ii) ^{230}Th/U dating of post-depositional, secondary calcite flowstone and subaerial microbialites at the underside of the boulders; and (iii) surface exposure dating of overturned boulders via ^{36}Cl concentration measurements in corals. Approaches (ii) and (iii) have never been applied to coastal boulder deposits so far. The three ^{14}C age estimates are older than 40 ka, i.e. most probably beyond the applicability of the method, which is attributed to post-depositional diagenetic processes, shedding doubt on the usefulness of this method in the local context. The remarkably convergent ^{230}Th/U ages, all pointing to the Late Holocene period (1.0–1.6 ka), are minimum ages for the transport event(s). The microbialite sample yields an age of 1.23 ± 0.23 ka and both flowstone samples are in stratigraphic order: the older (onset of carbonate precipitation) and younger flowstone layers yield ages of 1.59 ± 0.03 and 1.23 ± 0.03 ka, respectively. Four coral samples collected from the topside of overturned boulders yielded similar ^{36}Cl concentration measurements. However, the computed ages are affected by large uncertainties, mostly due to the high natural chlorine concentration. After correction for the inherited component and chemical denudation since platform emergence (inducing additional uncertainty), the calculated ^{36}Cl ages cluster between 2.5 ± 1.3 and 3.0 ± 1.4 ka for three of four boulders whilst the fourth one yields an age of 6.1 ± 1.8 ka, probably related to a higher inheritance. These ^{230}Th/U and ^{36}Cl age estimates are coherent with a suggested tsunami age of < 3.3 ka obtained from the investigation of allochthonous shell horizons in sediment cores of northwestern Bonaire. Whilst ^{230}Th/U dating of post-depositional calcite flowstone appears to be the most robust and/or accurate approach, these results illustrate the potential and current limitations of the applied methods for dating the dislocation of supralittoral boulders in carbonate-reef settings.

1. Introduction

Fields of dislocated boulders and blocks are amongst the most impressive sedimentary evidence of catastrophic coastal flooding events (Scicchitano et al., 2007; Frohlich et al., 2009; Goto et al., 2010; Etienne et al., 2011; Engel and May, 2012; Terry et al., 2013; May et al., 2015a); they are widely used to infer the most extreme magnitudes of marine flooding (tsunamis, storm surges) over Holocene time scales

* Corresponding author.
E-mail address: grixhon@uni-koeln.de (G. Rixhon).

http://dx.doi.org/10.1016/j.margeo.2017.03.007
Received 9 September 2016; Received in revised form 15 March 2017; Accepted 17 March 2017

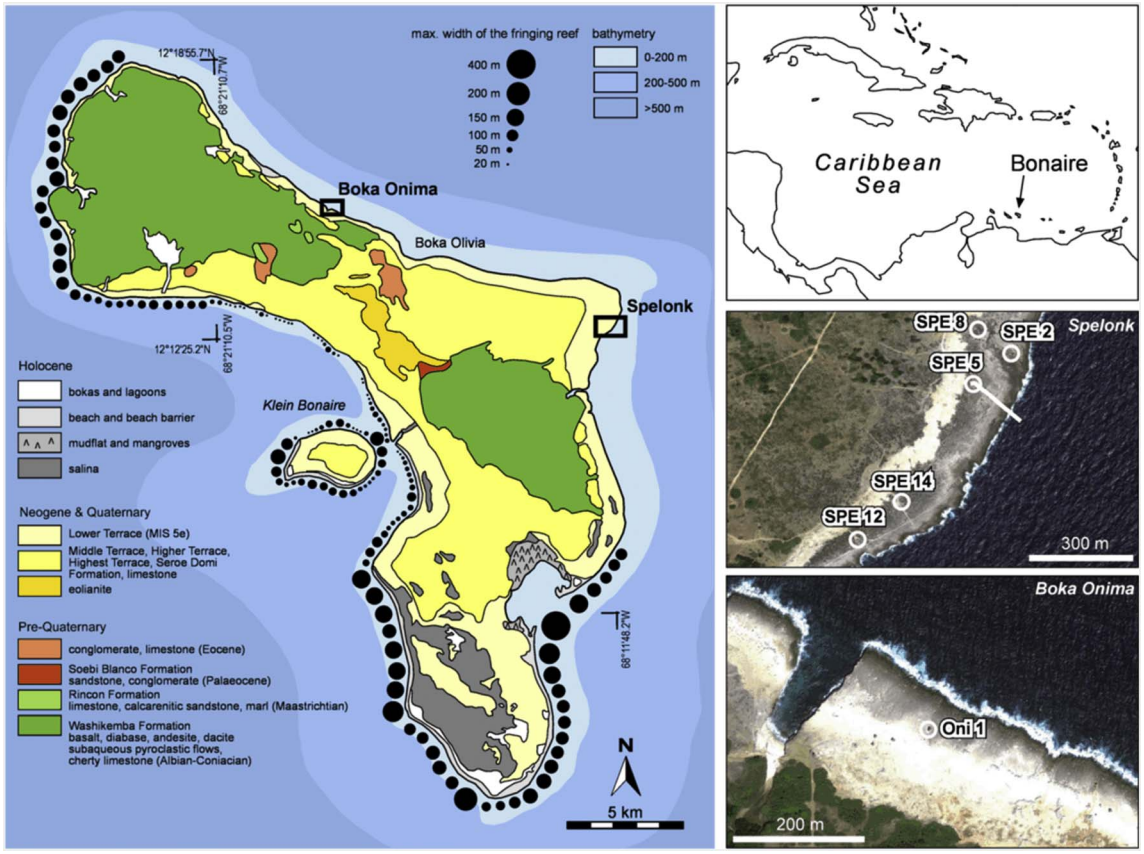

Fig. 1. Simplified geological map of Bonaire (left) (based on Pijpers, 1933; Westermann and Zonneveld, 1956; De Buisonjé, 1974) showing the study sites, offshore bathymetry (Scheffers, 2005) and the distribution of fringing reefs (Scheffers et al., 2006). The island's location in the Caribbean basin is indicated in the upper right. Two satellite images (Google Earth/ WorldView-2, 18 Jan 2011) show the spatial distribution of studied boulders at Spelonk (middle right) and Boka Onima (lower right).

(Etienne et al., 2011; Engel and May, 2012; Terry et al., 2013) and can potentially be used for coastal hazard assessment and planning (Miller et al., 2014). Besides the ongoing debate on and the continued challenges in distinguishing between hydrodynamic processes (tsunamis or storms, see Goto et al., 2010; Lorang, 2011; May et al., 2015b), dating the time of boulder dislocation is crucial for reconstructing magnitude-frequency relationships and, in particular, recurrence rates of extreme wave events. Whilst the use of optically stimulated luminescence (OSL) and radiocarbon (^{14}C-AMS) dating techniques are widely applied in the context of fine sediment records (e.g. Cisternas et al., 2005; Brill et al., 2012; Prendergast et al., 2012; Engel et al., 2013; May et al., 2015b), the dating of wave-emplaced blocks and boulders is still a challenge (Terry et al., 2013; Engel et al., 2016), wherefore the interpretation of the coarse-clast record suffers from significant limitations.

The timing of Holocene boulder transport is usually obtained through dating of attached marine organisms by ^{14}C-AMS (e.g. Scheffers et al., 2009; Barbano et al., 2010; Biolchi et al., 2016). In reef settings, dislodged coral clasts themselves may be dated by ^{230}Th/U and electron spin resonance (ESR) (e.g. Scheffers et al., 2014; Terry and Etienne, 2014) assuming that living corals are entrained during the transport events. However, Scheffers et al. (2014) illustrated the inevitable uncertainties and limitations related to this approach on Bonaire using a large dataset of ~400 ESR, ^{230}Th/U and ^{14}C ages from supratidal coral material (i.e. ridges, ramparts and boulders). The data show a rather uniform distribution of ages between 4200 and 2800 years BP and some clustering around 1500 as well as 500 years BP. A mid- to late Holocene age for the transport event(s) could be consequently inferred, even though it still remains questionable (i) if one or several events occurred and (ii) if the dated death of the corals coincides with the flooding event or if reworking plays a major role. The coral rubble ridges, ramparts and the solitary boulders may have a complex, long-term history of stepwise transport, accumulation, and modification during several strong storms and tsunamis (Morton et al., 2008; Scheffers et al., 2014).

Against the framework of these uncertainties, alternative dating techniques are required, especially those addressing the problem of reworking. Recently, palaeomagnetism was used to unravel the transport time of tsunamigenic coral boulders in Japan, although this method suffers from intrinsic limitations (Sato et al., 2014). Here, in addition to new ^{14}C dating of boring bivalves (*Lithophaga* sp.) attached to the boulders, we therefore applied first ^{230}Th/U dating of post-depositional, secondary calcitic flowstones and subaerial microbialites at the underside of the boulders. These data provide minimal ages for boulder dislocation and transport. Second, surface exposure dating based on cosmogenic ^{36}Cl measurements of overturned coral boulders may estimate the timing of dislocation and tsunami-induced transport on the reef platform. ^{36}Cl surface exposure dating has been applied to calcite-bearing boulders lying at or protruding from the surfaces of, for instance, moraines (e.g. Phillips et al., 1990), alluvial fans (e.g. Frankel et al., 2007) or landslide deposits (e.g. Prager et al., 2009), although potential effects of inheritance and/or post-depositional weathering must be carefully taken into account (Balco, 2011; Schmidt et al., 2011). Here, we adapted a sampling strategy recently developed to consider this issue for fluvially transported, overturned boulders during flood events (Fujioka et al., 2014). We also stress that this study represents a first attempt to apply ^{36}Cl surface exposure dating in the context of wave-transported coarse-clast deposits. Moreover, except for the pioneering study of Lal et al. (2005) presenting some ^{36}Cl measurements in coral-reef platforms of Barbados and Puerto Rico, aragonitic or calcitic corals were hitherto not investigated for cosmogenic nuclide analysis. Therefore, it is necessary to thoroughly present

and discuss the sampling strategy and the significance of the ^{36}Cl results. This study as a whole eventually aims to present and discuss the potential and current limitations of each of these three techniques in this specific littoral environment and to provide useful recommendations for potential applications in coastal geomorphology and sedimentology.

2. Physical setting

Coarse-clast records of several Caribbean islands were studied in the last decades in order to decipher past tsunami and/or hurricane occurrences (e.g. Jones and Hunter, 1992; Morton et al., 2006; Khan et al., 2010; Buckley et al., 2012). Comprising extensive supralittoral block and boulder fields as well as circumlittoral coral rubble ridges and ramparts, Bonaire's (Leeward Antilles) sedimentary inventory represents one of the most-studied coarse-clast records for extreme wave events in the Caribbean (Scheffers, 2002, 2004, 2005; Scheffers and Scheffers, 2006; Scheffers et al., 2014; Morton et al., 2006, 2008; Spiske et al., 2008; Watt et al., 2010; Engel and May, 2012).

Bonaire is part of the ABC Islands of the Lesser Antilles. It consists of a core of Upper Cretaceous volcanic rocks overlain by dolostones, marlstones and fossiliferous limestone and surrounded by a sequence of uplifted Pleistocene reef terraces (Fig. 1, Jackson and Robinson, 1994; Schellmann et al., 2004; Scheffers, 2005). The lowermost Marine Isotopic Stage (MIS) 5.5 terrace (Lower Terrace [LT]) – an age recently confirmed by Felis et al. (2015), Brocas et al. (2016), and Obert et al. (2016) – reaches a maximum width of 600 m and an elevation between 3 and 6 m above present mean sea level (a.s.l.) along the northeast coast, including our study sites Spelonk and Boka Onima (Figs. 1, 2a). It has a rugged limestone topography with rock pools along the terrace edges and notches and benches along the limestone cliffs (Fig. 2a, Scheffers, 2005).

At Spelonk, the LT is c. 3.5 m high. A rock pool zone at the cliff edge with high bioabrasive activity merges into a moderately karstified surface. A zone of up to 65 m inland is kept sediment-free. Up to 80 m from the cliff edge, fine to medium boulders are wedged into solution cavities. From c. 80–250 m, blocks and boulders are distributed over the LT (Fig. 2a), which is covered by a very poorly sorted sheet of sand to fine boulders and coral debris (thickness > 10 cm) containing many marine gastropod shells. The sand fraction hosts an initial soil horizon (Engel and May, 2012). Near Boka Onima, the LT has an elevation of c. 5 m. A previous broad polymodal ridge complex (Scheffers, 2002) has been mined recently and only singular large boulders remain on the sand-covered platform at various distances to the cliff edge.

The largest singular boulders identified to have been moved during recent hurricanes weigh from 1 up to 9 t (Engel and May, 2012). Those remaining immobile during these events and for which tsunami deposition is likely, weigh up to 150 t (Scheffers, 2002, 2005; Watt et al., 2010; Engel and May, 2012). The source of most of the boulders was identified as the receding cliff edge (Fig. 2b), exemplified by a smaller boulder at Boka Olivia (Fig. 1), which was quarried and transported during a recent storm event, leaving impact marks on top of the karstified platform during rolling/saltation (Engel and May, 2012). Clasts investigated in this study (Table 1) belong both to boulders (from 0.25 to 4.1 m) and megaclasts (> 4.1 m), according to the grain size classification of Blair and McPherson (1999). For clarity, all clasts will be named boulders hereinafter.

3. Methods

Three distinct methods are implemented in this study to constrain the timing of boulder transport on Bonaire (Table 1): (i) ^{14}C-AMS dating of *Lithophaga* sp. remains preserved in their boreholes inside the boulders (3 samples), (ii) ^{230}Th/U dating of post-depositional calcitic flowstones (2 samples) and subaerial microbialites (1 sample), formed at the underside of the boulders through secondary carbonate precipitation; and (iii) surface exposure dating of overturned boulders via ^{36}Cl concentration measurements in corals (6 samples). Thin section as well as X-ray diffraction (XRD) and fluorescence (XRF) analyses were also performed to investigate the internal structure and composition of some samples.

3.1. Thin sections and XRD/XRF analyses

Thin sections were prepared from the flowstone and microbialites samples SPE 12 U1 and ONI 1 U, respectively, whose sub-samples for ^{230}Th/U dating were taken from (see Section 3.3). They allow identifying the most suitable areas for the extraction of dating material in these samples. The latter were impregnated with resin and cut into 28 × 48 mm and 35 × 120 mm large blocks. Thin sections (15–25 µm) were polished and covered with a coverslip. The thin sections were visually analysed using a polarising petrographic microscope under

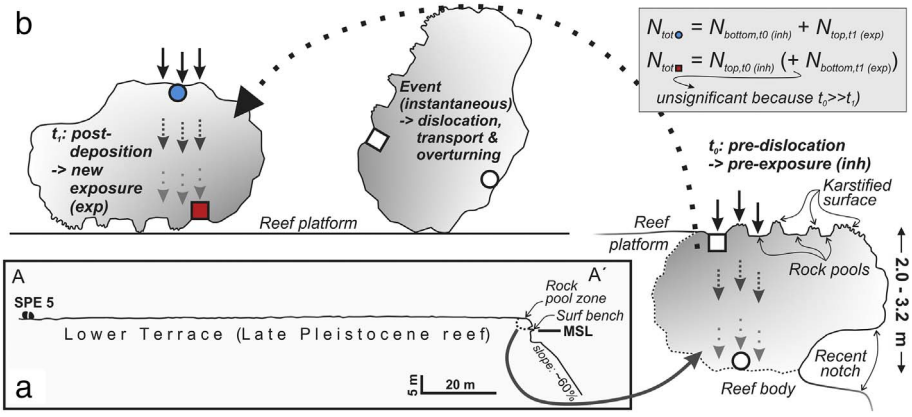

Fig. 2. a) Cross-section of the lower terrace at Spelonk (see Fig. 1 for location) showing the position of one boulder sampled in this study (SPE 5, see Table 1) (adapted from Engel and May, 2012). b) Sampling strategy for ^{36}Cl surface exposure dating: only boulders having experienced complete overturning during transport were sampled. Such an overturn is unequivocally attested by former surface rock pools (t_0), now located on the bottom side of the boulders (t_1) and by bio-erosive notches (t_0), now exposed on the top side of the boulders (t_1). Blue circle and red square refer to sampling positions at both sides of the boulder. The three downward-oriented arrows (full black to dotted gray) symbolize the decreasing intensity of the cosmic-ray flux, hence the ^{36}Cl production rate, from the top to the base of the boulder.Note that, despite the significant thicknesses of the sampled boulders (varying from 2 to 3.2 m), the production at the base is still substantial. Cosmogenic inventories at both sides of overturned boulders are thus accumulated during the two stages prior and after the instantaneous transport event. Total concentration of the currently exposed side ($N_{tot,blue\ circle}$ in atoms/g) is the sum of exposition at depth during t_0 (i.e. the inherited component, $N_{bottom,t0}$), and exposition at the surface during t_1 ($N_{top,t1}$). Total concentration of the currently shielded side ($N_{tot,red\ square}$) may be assimilated to the inherited component from exposure at the surface during t_0 ($N_{top,t0}$) as the concentration accumulated at depth after the transport event ($N_{bottom,t1}$) is negligible ($t_0 \gg t_1$). (For interpretation of the references to color in this figure legend, the reader is referred to the web version of this article.)

Table 1
Main characteristics of the six investigated boulders on Bonaire and the thirteen samples collected for ^{14}C dating (three samples), $^{230}Th/U$ dating (four samples) and ^{36}Cl surface exposure dating (six samples).

Boulder	Lat (°N)/long (°W)	Elevation (m a.s.l.)	Boulder maximum length & thickness (a- & c-axis)	Sample ID	Dating method	Sample nature	Sample thickness (cm)	Density of sampled material	Boulder bulk density	Grain size used (μm)	Comments
ONI 1	12.2532/ 68.3089	6.0	5.2–2.2	ONI 1 U-A	$^{230}Th/U$	Reef rock	0.2	–	–	–	Calcarenitic surface of boulder ONI 1 (Fig. 5c)
				ONI 1 U-B	$^{230}Th/U$	Microbialite	0.4	–	–	–	Subaerial microbialites developed at the bottom side (former rock pool) of the boulder (Fig. 5b–e)
SPE 2	12.2101/ 68.1976	5.0	4.1–1.95	SPE 2 R	^{14}C	Boring bivalve: *Lithophaga* sp.	–	–	–	–	Well preserved boring cavity (Fig. 3)
SPE 5N	12.2093/ 68.1987	6.5	4.7–3.2	SPE 5N R1	^{14}C	Boring bivalve: *Lithophaga* sp.	–	–	–	–	Well preserved boring cavity (Fig. 3)
				SPE 5N R2	^{14}C	Boring bivalve *Lithophaga* sp.	–	–	–	–	Well preserved boring cavity (Fig. 3)
				SPE 5N Cl1	Surface exposure[a]	Coral: *Acropora palmata*	1.5	2.3–2.4	2.07	250–500	Top surface of the boulder (Supplementary material 2)
				SPE 5N Cl2	Surface exposure[a]	Coral: *Montastrea* sp.	4.5	1.4–1.5	2.07	250–500	Top surface of the boulder (Supplementary material 2)
SPE 8	12.2107/ 68.1985	6.1.	9.1–2.8	SPE 8 Cl	Surface exposure[a]	Coral: *Acropora palmata*	2.0–3.0	2.3–2.4	2.35	250–500	Top surface of the boulder (Supplementary material 2)
SPE 12	12.2052/ 68.2017	6.0	5.2–2.2	SPE 12 Cl	Surface exposure[a]	Coral: *Acropora palmata*	1.5–2	2.3–2.4	2.20–2.25[b]	125–250	Top surface of the boulder (Fig. 4g)
				SPE 12 U1-A	$^{230}Th/U$	Flowstone	0.2	–	–	–	Downward-oriented, elongated flowstone (Fig. 4b–f)
				SPE 12 U1-B	$^{230}Th/U$	Flowstone	0.2	–	–	–	Downward-oriented, elongated flowstone (Fig. 4b–f)
SPE 14	12.2062/ 68.2001	5.5	5.2–2.0	SPE 14 Cl1	Surface exposure[a]	Coral: *Acropora palmata*	2.0–2.5	2.3–2.4	2.20–2.25[b]	250–500	Top surface of the boulder (Supplementary material 2)
				SPE 14 Cl2	Surface exposure[a]	Coral: *Acropora palmata*	2.0	2.3–2.4	2.20–2.25[b]	125–500	Bottom surface of the boulder (Supplementary material 2)

[a] Surface exposure dating: neither topographic shielding nor surface inclination (i.e. self-shielding) to account with for any boulder. The superficial weathering rind of corals, ranging between 0.1 and 4 cm, was removed before sample processing (see Supplementary material 3).
[b] Average density of the coral reef boulders on Bonaire.

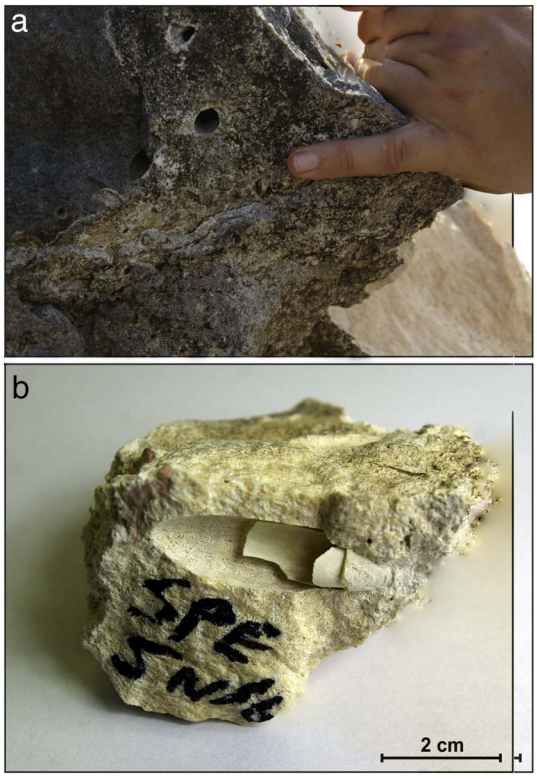

Fig. 3. Boring bivalves (*Lithophaga* sp.) sampled for ^{14}C dating from boulders SPE 2 and SPE 5N. a) Fresh-looking boreholes; note boring bivalve still present in the hole. b) Rock sample with cavity and bivalve collected from SPE 5, radiocarbon-dated to > 40,000 cal BP (see Table 2).

both plane polarised light (PPL) and crossed-polarised light (XPL). In addition, XRD and XRF analyses were conducted on the microbialitic sub-sample ONI 1 U-B to investigate its mineralogical and inorganic element compositions. For XRD, ground sampling material was introduced into a powder X-ray diffractometer (Siemens D 5000) with 10 s/point step size and 0.05° steps. A fixed 1° divergence slit and antiscatter was used at diffraction angles from 5 to 75° 2θ. The Cu K-alpha radiation source was operated at 40 keV and 40 mA. The data were analysed with DiffracPlus Eva software package (Bruker AXS). For XRF, a NITON XL3t X-Ray fluorescence (XRF) handheld scanner (Analyticon Instruments) was used. Semi-quantitative variations of elements were analysed by scanning ground and compressed sample material (< 2 mm) for 160 s. Element amounts are represented in parts per million (ppm) and estimate relative concentrations in the ground sample material.

3.2. Radiocarbon dating

Three partly preserved bivalve shells of *Lithophaga* sp. were found inside fresh-looking boring holes in two of the boulders (SPE 2 R, SPE 5N R1 and R2) at Spelonk (Fig. 3; Table 1) and were collected for ^{14}C-AMS dating at the 14CHRONO Centre, Queens University Belfast, UK. Calib 7.0 software and the Marine13 dataset (Reimer et al., 2013) were used for calibration. A local reservoir effect of ΔR = 25 ± 45, based on six *Diploria strigosa* fragments dated by ^{230}Th/U and ^{14}C, was used (Scheffers et al., 2014).

3.3. ^{230}Th/U dating

3.3.1. Sample collection

Based on our field observations, slightly < 50% of the large reef-top boulders displayed occurrences of calcite flowstones and/or fossil microbialites and active microbial mats. At Spelonk, flowstones are attached to the bottom surface of some boulders. On boulder SPE 12, an elongated flowstone of c. ~40 cm length, indicating a post-depositional formation due to its specific growth pattern associated with dripping water (Fig. 4a, b), was selected for further investigations. Evidence for carbonate dissolution was observed directly above the flowstone, where rain water draining the block surface overflows the edge of the boulder (Fig. 4a). This dissolution/precipitation pattern on SPE 12 strongly points to boulder stability since its deposition, thereby precluding any further reworking after transport and overturning (Fig. 4a, b). The middle section of the flowstone was sampled using a rock saw, and a 3 cm-long section of the flowstone was analysed in the lab (SPE 12 U1; Fig. 4b, c; Table 1). The inner part of sample SPE 12 U1 contains the calcarenitic surface of block SPE 12 (Fig. 4d). Directly above the calcarenitic base of the boulder, two subsamples were collected from the lower part of the sample (SPE 12 U1-A, SPE 12 U1-B; Fig. 4e, f). The thickness of all samples ranged between 2 and 4 mm (Table 1).

In addition both fossil microbialites and active microbial mats are attached to the surface of a former rock pool at the underside of the boulder at ONI 1 (see Fig. 5a–b and Supplementary material 1). Microbialites are rather common in the near shore environment (e.g. coastal wetlands) of regions characterised by a warm climate (Saint Martin and Saint Martin, 2015), including for instance coastal areas of Venezuela, neighbouring our study area of Bonaire. Active rock pools at the cliff's edge represent a highly dynamic environment, fairly unsuited for the growth of microbial mats and microbialites. Instead, these microorganisms on Bonaire are found in an analogous moist, shielded setting than that of emerged sea caves on Hawaï described by Léveillé et al. (2000), where carbonate microbialites develop in relation to freshwater seeping spots in the cave ceiling. Whilst a post-depositional formation of these microbialites is thus highly probable, both inactive and active microorganisms in the same former rock pool point to boulder stability since its deposition. A hand specimen of dry microbialite was sampled, exhibiting an irregular and knobby surface texture (ONI 1 U; Fig. 5b–c). The base of the sample ONI 1 U reaches the calcarenitic surface of the boulder ONI 1 (Fig. 5c). Subsamples for ^{230}Th/U dating were collected from the basal reef rock (ONI 1 U-A) and the central part of the attached microbialite (ONI 1 U-B) (Fig. 5c–e).

3.3.2. Sample preparation and laboratory measurements

The flowstone (SPE 12 U1) and microbialite (ONI 1 U) samples were cut along their growth axes and subsamples for ^{230}Th/U dating were taken using a diamond-coated band saw. The methods of sample preparation and mass spectrometric analysis follow the procedure of Douville et al. (2010). Measurements were performed with an ICAP Q inductively coupled plasma/mass spectrometer (iCAP Q ICP-MS, Thermo Scientific) at the Institute for Environmental Physics, Heidelberg. Ages were calculated using the half-lives of Cheng et al. (2000). Correction for detrital contamination assumes a ^{232}Th/^{238}U weight ratio of 3.8 ± 1.9 and ^{230}Th, ^{234}U and ^{238}U in secular equilibrium. Age uncertainties are quoted at the 2σ-level and do not include half-life uncertainties.

3.4. ^{36}Cl surface exposure dating

3.4.1. Sampling strategy

Some of the tsunamigenic boulders at Boka Spelonk were deposited in upside-down position after transport (Engel and May, 2012). This complete overturn is unequivocally indicated by rock pools now located on the bottom side of the boulders, and by bio-erosive notches, now exposed on the top side (Figs. 2, 4a, 5a). Consequently, the boulders exhibit a formerly incompletely shielded side, which became exposed at the surface after the transport event, and an opposite side, which was formerly exposed at a palaeosurface and which became incompletely shielded after the transport event, similar to the boulders described by Fujioka et al. (2014). Although subsurface ^{36}Cl production rates exponentially decrease with depth (e.g. Braucher et al., 2011), produc-

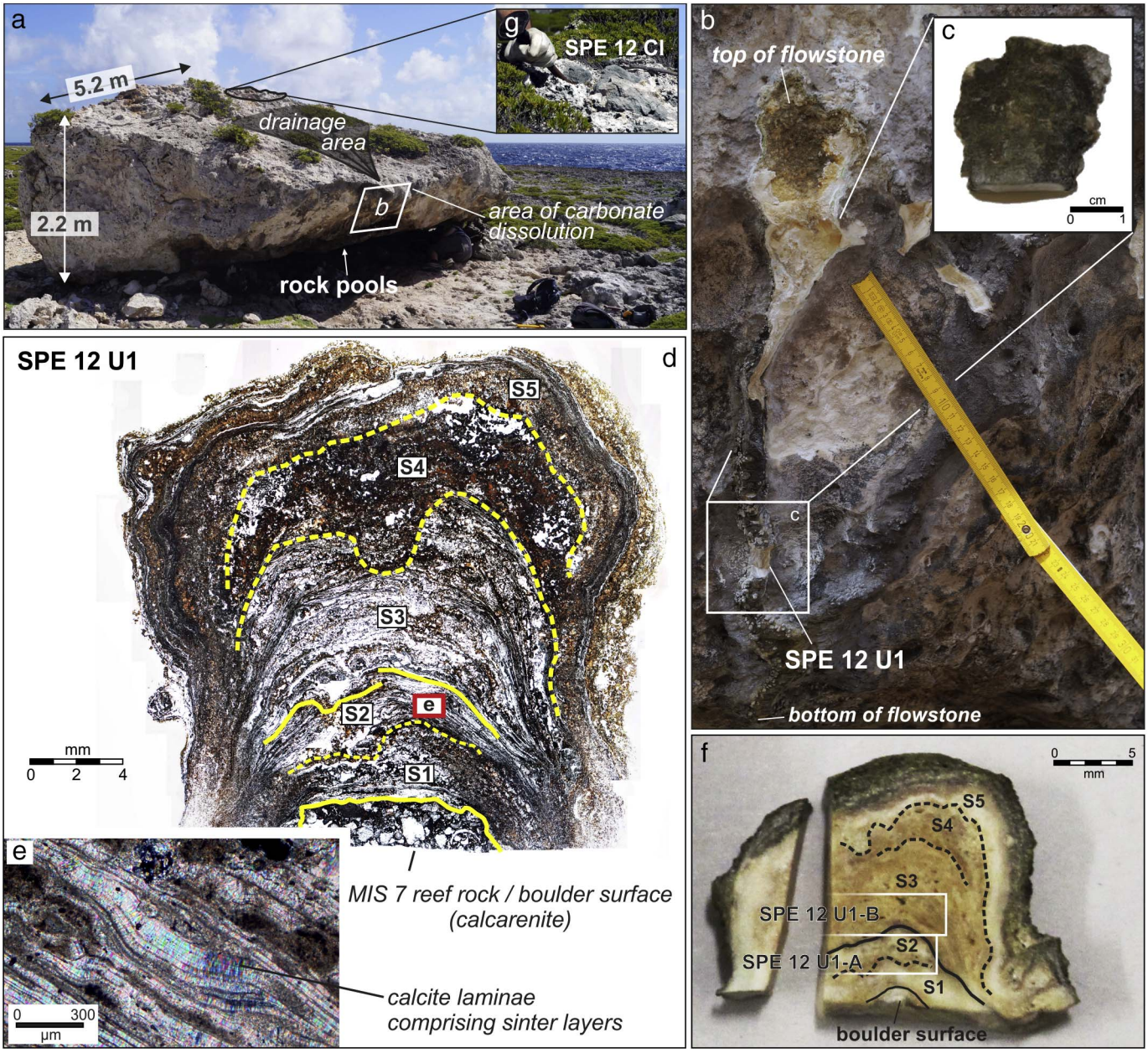

Fig. 4. a) Setting and sampling of the overturned boulder SPE 12, indicated by well-developed rock pools at the bottom side. b, c) A 3 cm-long section was collected from a downward-facing, elongated flowstone (~40 cm) attached to the southern side of the boulder. d) Assemblage of microscopic images: the basal part of sample SPE 12 U1 contains the calcarenitic surface of boulder SPE 12 (i.e., MIS 7 reef rock; see Supplementary material 6), whereas S1 to S5 refer to assumed different generations of carbonate precipitation, partly characterised by organic remains and a red-brown color (micro-organisms). e) Detail of a small subsection of layer S2; note the secondary calcite precipitation (laminae). f) Two subsamples were collected from the lower part of the sample for ^{230}Th/U dating, i.e. directly above the calcarenitic base of the sample (SPE 12 U1-A and B). S1 was not sampled to avoid contamination with older reef rock material. g) Top surface of the boulder and sampling of *Acropora palmata* (SPE 12 Cl). (For interpretation of the references to color in this figure legend, the reader is referred to the web version of this article.)

tion at those depths corresponding to the thicknesses of the sampled boulders (see Table 1) is still significant and varies between 10 and 16% of the ^{36}Cl production at the surface, depending on the composition and density of boulders. Therefore, the cosmogenic inventory at the currently exposed side has accumulated during the two stages prior (t_0) and after (t_1) the transport event (*instantaneous*), the new exposure time span (t_1, i.e. Holocene to present) being much shorter than the pre-dislocation time span (t_0, i.e. MIS 5.5 to Holocene). Total concentration of the currently exposed side (N_{tot}) is the sum of exposition at depth during t_0 (i.e. the inherited component, $N_{bottom,t0}$ in atoms/g), and exposition at the surface during t_1 ($N_{top,t1}$ in atoms/g, see Fig. 2b). As this last component is of interest here, we must assess the inherited component at depth. According to Fujioka et al. (2014), this can be achieved using the concentration of the currently shielded (and formerly exposed) side of the boulder, where the cosmogenic inventory consists (almost) exclusively of the inherited component from exposure at the surface during t_0 ($N_{top,t0}$, because $t_0 \gg t_1$):

$$N_{bottom,t0} = N_{top,t0}.\ e^{-(\rho.x/\Lambda)} \quad (1)$$

where ρ and x denote the bulk density and the thickness of the boulder, respectively, and Λ the spallation attenuation length (g/cm^2).

To minimize the influence of inheritance (i.e. $N_{bottom,t0}$) as much as possible, only the thickest (≥ 2 m) boulders (Table 1), displaying clear evidence of a complete overturning, were sampled for ^{36}Cl dating. The same reasoning holds for the reworking problem: only the largest and

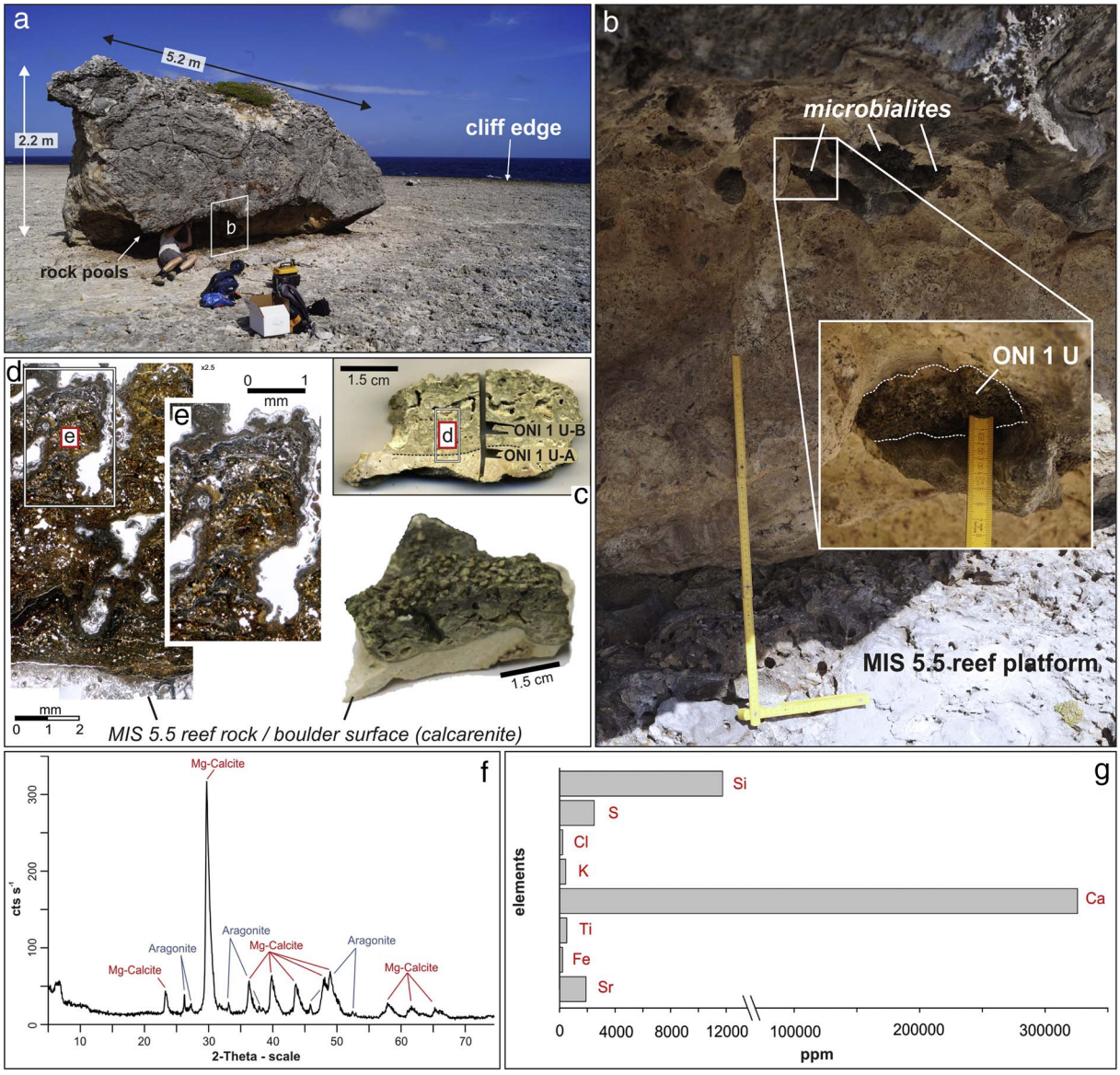

Fig. 5. a) Setting and sampling of the overturned boulder ONI 1, indicated by well-developed rock pools at the bottom side. b, c) A stock of subaerial microbialites was found at the surface of a former rock pool and sampled for ^{230}Th/U dating (ONI 1 U). Carbonate microbialites were found in protected locations of the former rock pool, partly related to freshwater seeping.Note the irregular and knobby surface texture of the sample. Subsamples for ^{230}Th/U dating were collected from the basal reef rock (ONI 1 U-A) and the central part of the attached microbialites (ONI 1 U-B). d, e) Microscopic image: the microbialite is characterised by an amorphous, brown matrix without any evident organization. Large pores or hollows occur due to its nodular texture. f) XRD: the peaks (counts s^{-1}) show that the microbialitic material is essentially formed of Mg-calcite and aragonite. g) XRF: element composition reveals a clear predominance of Ca and the presence of Si, S, Cl, K, Ti, Fe and Sr in various concentrations (Mg: not measured). (For interpretation of the references to color in this figure legend, the reader is referred to the web version of this article.)

heaviest boulders, for which any post-depositional reworking seems fairly unlikely, were selected. Six coral samples were collected with hammer and chisel from four distinct boulders at Spelonk (Table 1; see also Supplementary material 2): five samples from the current top side, i.e. SPE 5N Cl1 & Cl2, SPE 8 Cl, SPE 12 Cl (Fig. 4g), SPE 14 Cl1, and one from the current bottom side, i.e. SPE 14 Cl2. Coral species of all samples consist of *Acropora palmata*, except one sample: to test the possible effect of density variability, we collected one sample of *Acropora palmata* (SPE 5N Cl1, ρ: 2.3–2.4 g/cm^3) and one of *Montastrea* sp. (SPE 5N Cl2, ρ: 1.4–1.5 g/cm^3) from the same location (Table 1; see also Supplementary material 2).

3.4.2. Sample preparation

The samples were prepared at the Institute of Geology and Mineralogy in Cologne following mainly the chemistry protocol of Stone et al. (1996). First, the outer weathering rind and any trace of contamination such as calcite recrystallization were removed in order to obtain thin slabs (1.5 to 4.5 cm-thick) of fresh-looking coralline matrix for crushing and sieving (see Supplementary material 3). Each sample was rinsed and leached twice in 0.3 M HNO_3 until ~13% of the material was removed. The samples were spiked with a known amount of isotopically enriched stable chloride carrier (isotope dilution) to allow simultaneous determination of the natural chlorine and ^{36}Cl (Desilets et al., 2006 and references therein). After the addition of the chlorine carrier and some excess $AgNO_3$ to avoid degassing, ~42 g of each sample were dissolved using MilliQ water and subsequent careful addition of 2 M HNO_3. ^{36}Cl's isobar ^{36}S was concurrently removed through the precipitation of $BaSO_4$ to reduce interference in the ^{36}Cl counting during the subsequent Accelerator Mass Spectrometer (AMS) measurements. Finally, chlorine was precipitated as AgCl and the samples were measured at the CologneAMS facility.

A chemistry blank is coupled with each series and measured in the

same AMS run to track any stable chlorine contamination in the chemistry process. To ensure the accuracy and precision of the AMS measurement, the machine was calibrated and normalized to three different concentrated standards ($^{36}Cl/Cl$: 5.000×10^{-13}, 1.600×10^{-12}, and 1.000×10^{-11}) from the NIST SRM 4843 material (Sharma et al., 1990). For each AMS measurement, we additionally prepared two pure spike blanks (Oak Ridge National Laboratory batch 150301, NaCl enriched with ^{35}Cl), and two blanks with the $^{35}Cl/^{37}Cl$ natural ratio of 3.127 (Standard Reference Material 975 and a commercial NaCl purchased from VWR company). Major and trace element contents of bulk non-leached sample material were measured by fusion inductively coupled plasma and fusion mass spectrometry at Actlabs (Canada) to calculate the sample specific production rate of ^{36}Cl (see Supplementary material 4). Additionally an aliquot of each dissolved sample was analysed on the ICP-OES at the Institute of Geology and Mineralogy in Cologne to reveal the composition of the target AMS-measured fraction.

4. Results

4.1. Thin section and XRD/XRF analyses

At the base of both rock samples chosen for $^{230}Th/U$ dating (SPE 12 U1, ONI 1 U), a heterogeneous carbonate sandstone (calcarenite) was documented (Figs. 4–5). In all cases, the calcarenite is characterised by up to 1 mm large mollusk and coral fragments which constitute and/or are embedded in a sandy matrix. The calcarenite represents the boulders' original surface, i.e. – most likely – a section of the former MIS 5.5 reef platform (Kim and Lee, 1999).

At the flowstone (SPE 12 U1), well-stratified units of calcitic material have accumulated in half-circular layers on top of the calcarenite core (Fig. 4d–f). Sections with clean and regular calcite crystals (particularly S1–S3, S5) alternate with rather amorphous, brown sections without any apparent internal organization (S4), the latter interpreted to represent organic remains. Well-laminated calcite layers especially occur in the lower/central part of the flowstone (S1–3, Fig. 4d–f).

In contrast, thin sections from the microbialite sub-sample (ONI 1 U-B) show an amorphous, brown matrix without visible lamination (Fig. 5d, e). Large pores or hollows occur due to the nodular texture of the microbialites (Fig. 5d, e). From the core section of the microbialite, XRD analysis highlights several main Mg-calcite and aragonite peaks (Fig. 5f). XRF analysis shows an element composition clearly dominated by Ca, accompanied by Cl, Fe, K, S, Si, Sr and Ti present in various concentrations (Fig. 5g). The presence of sulphur is consistent with the very thin coating of secondary gypsum occurring along the pore margins (J. Braga, pers. communication). Although the secondary Mg-calcite precipitation of microbialites seems to contain more impurities than the well-laminated calcite layers of SPE 12 U1, it is relevant to compare both kinds of material for $^{230}Th/U$ dating.

4.2. Radiocarbon ages

AMS-^{14}C dating of the three boring bivalves from the boulders SPE 2 and SPE 5N yield comparable ages of 41.37 ± 1.32 (SPE 2 R), 44.98 ± 2.70 (SPE 5N R1) and 39.58 ± 1.23 (SPE 5N R2) ka cal BC (Fig. 6; Table 2).

4.3. Uranium-thorium ages

Whilst the lowermost flowstone unit (S1) was not sampled to avoid contamination with older material from the calcarenitic core of the boulder, the flowstone layers S2 and S3 (samples SPE 12 U1-A and B; see Fig. 4f) yield uncorrected ages of 1.63 ± 0.01 and 1.29 ± 0.01 ka, respectively (Table 3). After correction for detrital Th, these ages slightly changed to 1.59 ± 0.02 and 1.23 ± 0.03 ka

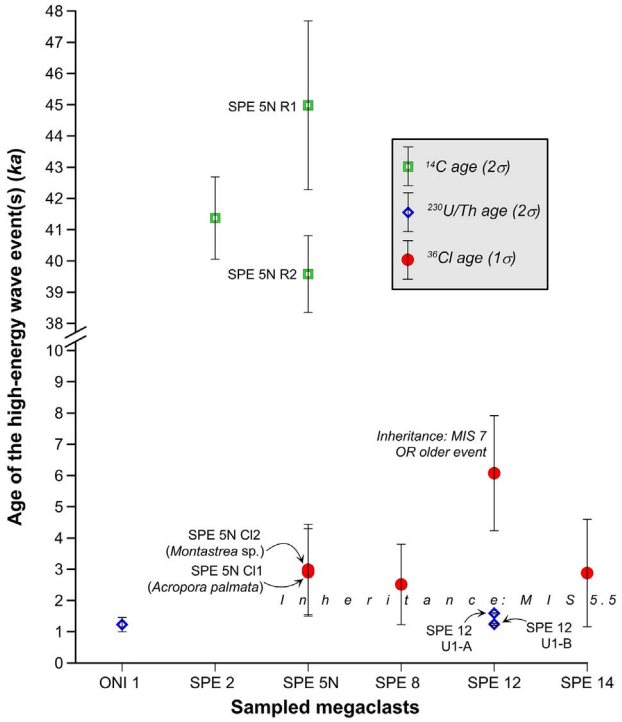

Fig. 6. Synthesis of age results obtained from the three dating methods.Note that ^{14}C ages of *Lithophaga* sp. are inappropriate to constrain the timing of dislocation and transport of the Holocene event (significant age overestimation due to neomorphism, see text Section 5.1). The minimum ages obtained by $^{230}Th/U$ dating of secondary calcite flowstone (SPE 12) and subaerial microbialites (ONI 1) are in good agreement (1.0–1.6 ka). Though imprecise, ^{36}Cl ages of three overturned boulders at Spelonk cluster in the Late Holocene (2.5 ± 1.3 to 3.0 ± 1.4 ka), for which inheritance was corrected for pre-exposure (t_0) since the emersion of the MIS 5.5 platform (see Fig. 2). Independent $^{230}Th/U$ dating of boulder SPE 12 (see Supplementary material 6) suggests an older source area at the cliff's edge (MIS 7, see Fig. 8a): inheritance cannot be reliably constrained for this boulder since no sample was collected at its current shielded side. Sample SPE 12 Cl might thus result in an overestimated exposure age (see text Section 5.2).

(Fig. 6; Table 3). Sample ONI 1 U-A, collected from the calcarenitic boulder surface to which the microbialites are attached, yields a corrected age of 138.8 ± 1.3 ka (same as the uncorrected age, Table 3) and thus points to the cold-to-warm transition between MIS 6 and MIS 5.5. Sample ONI 1 U-B, collected from the central part of the microbialitic zone, yields an uncorrected age of 1.69 ± 0.02 ka (Table 3). The high ^{232}Th concentration of this sample imposes a significant age correction; the corrected age amounts to 1.23 ± 0.23 ka (Fig. 6; Table 3).

4.4. ^{36}Cl surface exposure ages

We used the Excel spreadsheet of Schimmelpfennig et al. (2009) to calculate both the sample specific production rate and the exposure ages. The following production rates were integrated in the spreadsheet: 52.2 ± 5.2 at/g/a for the spallation of calcium at sea level and high latitude (using the scaling of Stone, 2000), 117 at/g/a for the slow negative muon stopping rate, and 759 n/cm^2/a for production from low-energy neutron absorption from ^{35}Cl (Marrero et al., 2016; see also Supplementary material 5).

Stable chlorine concentrations of the samples are high and range from 292 ± 30 to 421 ± 45 µg/g (Table 4). This results in large ^{36}Cl concentration uncertainties, ranging from 11 to 17% (see Section 5.2). The number of Cl and ^{36}Cl atoms in the blank were subtracted from the number of Cl and ^{36}Cl atoms in the samples. This resulted in a decrease of the uncorrected ^{36}Cl concentrations ranging from 0.4 to 3.9%. Amongst the five samples from the current top surfaces of boulders,

Table 2
^{14}C dating results of the three samples collected from SPE 2 and SPE 5N.

Sample ID	^{14}C age BP (yr) (2σ)	^{14}C age cal BC (yr) (2σ)	d^{13}C	F^{14}C	2σ uncertainty	uAC
SPE 2 R	39,376 ± 859	41,370 ± 1319	− 1.4	0.0074	0.0008	29.3
SPE 5N R1	43,329 ± 1443	44,975 ± 2699	2.0	0.0045	0.0008	31.5
SPE 5N R2	37,241 ± 688	39,580 ± 1125	− 0.9	0.0097	0.0008	32.4

four show similar ^{36}Cl concentrations (N_{tot}): 1.97 ± 0.32 10^5 (SPE 8 Cl), 2.00 ± 0.33 10^5 (SPE 5N Cl1), 2.17 ± 0.35 10^5 (SPE 5N Cl2) and 2.40 ± 0.35 10^5 (SPE 14 Cl1) atoms/g, whilst the remaining one (SPE 12 Cl) shows a higher concentration (3.55 ± 0.38 10^5 atoms/g) (Fig. 7; Table 4). Concentrations of the two different coral taxa (*Acropora palmata* and *Montastrea* sp.) of boulder SPE 5N are in very good agreement. The concentration of the sample collected from the bottom side (SPE 14 Cl2) is the highest and amounts to 11.90 ± 1.30 10^5 atoms/g (Fig. 7; Table 4). This value is used to assess an inherited component at the currently exposed surface of boulder SPE 14 using Eq. (1).

According to the ^{230}Th/U dating of Obert et al. (2016), the LT of the eastern coast of Bonaire was formed during MIS 5.5 (120–130 ka) and the age of our sample ONI 1 U-A also points to the same time period (transition MIS 6 to MIS 5.5). We therefore assume that the corals forming the boulder field around SPE 14 are ~125 ka old and, since the overturning of these boulders occurred during the Holocene, the current bottom side of SPE 14 was previously exposed for ~120 ka (i.e. pre-dislocation exposure = t_0). Based on this assumption, the denudation rate of the LT since its emersion can be estimated from the concentrations measured in the coral sampled at the bottom side of boulder 14 (SPE 14 Cl2) using the spreadsheet of Schimmelpfennig et al. (2009). It amounts to 21 ± 5 mm/ka. As the boulders are all located in the same area, this denudation rate and the exposure duration for t_0 (~120 ka) is used to estimate the inherited component of all other ^{36}Cl samples. To do so, we reconstruct the depth profiles before the overturning event for each boulder using their respective thickness, i.e. their depth below the surface of LT prior to overturning, and the ^{36}Cl concentrations (Fig. 7).

The subtraction of the inherited ^{36}Cl concentration ($N_{bottom,t0[inh]}$) from the aforementioned concentration measurements (N_{tot}) yields the ^{36}Cl amount that is accumulated since the overturning event ($N_{top,t1[exp]}$; Fig. 2b). The nominal value of the latter for the samples SPE 5 Cl1, SPE 5 Cl2, SPE 8 Cl and SPE 14 Cl1 are very similar and amount to 0.72 ± 0.35 10^5, 0.81 ± 0.39 10^5, 0.67 ± 0.34 10^5 and 0.66 ± 0.39 10^5 atoms/g, respectively (Table 4). The calculated nominal ^{36}Cl concentration of SPE 12 Cl is higher and amounts to 1.42 ± 0.43 10^5 atoms/g (Table 4). Based on these concentrations, we calculate exposure ages since the overturning event of 2.9 ± 1.4 and 3.0 ± 1.4 (SPE 5), 2.5 ± 1.3 (SPE 8), 2.9 ± 1.7 ka (SPE 14) and 6.1 ± 1.8 ka for SPE 12 (Fig. 6; Table 4).

5. Discussion

5.1. Inadequacy of ^{14}C ages of boring bivalves

Radiocarbon dating of the three boring bivalves yield age estimates > 40 ka, which is very close to the upper age range of the dating method. Boulder transport at that time is very unlikely as (i) the sea level at that time was at least 80 m below the present one (Bard et al., 1990) and (ii) the ~400 exclusively mid- to late Holocene ages derived from coral clasts on the LT strongly indicate deposition atop the reef platform during the present sea-level highstand (Scheffers et al., 2014). We therefore suggest that the *Lithophaga* sp. organisms, all collected from fresh-looking holes bored into the supra-littoral boulders, had incorporated "old" $CaCO_3$ from the MIS 5.5 reef platform. This very common diagenetic process of post-mortem carbonate dissolution, recrystallization and replacement – predominantly from high-Mg calcite and aragonite to low-Mg calcite – is known as neomorphism and causes significant age overestimation (Douka et al., 2010). Consequently, within the framework of this study, these fossils are inappropriate for dating the dislocation of boulders during extreme wave events. Although it has been shown that ^{14}C dating on such boring bivalves may yield insightful results in comparable settings (e.g. Scheffers et al., 2009; Barbano et al., 2010), we recommend careful field examination and very critical result interpretation before drawing any age inference based on such data.

5.2. ^{36}Cl surface exposure ages: diverse sources of uncertainties

Ages for boulder overturning based on ^{36}Cl concentrations potentially have large uncertainties. Firstly, most of them are related to the high (and variable) amount of natural chlorine concentration in our samples (see Section 4.4.), from which two main implications arise. (i) A systematic consequence is that the measured ^{35}Cl/^{37}Cl ratios will be very close to the natural one, making the isotope dilution approach, hence the inferred Cl and ^{36}Cl concentrations, somewhat imprecise. (ii) The production rate of ^{36}Cl from thermal neutron capture by ^{35}Cl, which is associated with high uncertainties (e.g. Schimmelpfennig et al., 2009), significantly increases with increasing natural chlorine at the surface, and even more at shallow depth (e.g. Gosse and Phillips, 2001; Dunai, 2010). Whilst this issue only concerns the ^{36}Cl concentrations estimated for the exposure duration after the transport event

Table 3
^{230}Th/U dating results of the four samples collected from ONI 1 and SPE 12. All measurements were performed with ICAP Q and all uncertainties are given with 2σ. AR: activity ratio.

Sample ID	Lab no.	^{238}U (ng/g)	^{232}Th (ng/g)	^{230}Th/^{238}U AR	^{230}Th/^{232}Th AR	d^{234}U corr (error 2σ)	Uncorrected age (ka)	Corrected age[a] (ka)	d^{234}U (init.)
ONI 1 U-A	7416	2682.83 ± 0.90	0.6860 ± 0.0028	0.8083 ± 0.0032	9678.6 ± 55.4	105.1 ± 2.7	138.8 ± 1.3	138.8 ± 1.3	155.5 ± 4.1
ONI 1 U-B	7417	1366.80 ± 0.10	24.98 ± 0.045	0.0175 ± 0.0024	2.936 ± 0.030	143.3 ± 1.2	1.687 ± 0.02	1.23 ± 0.23	143.8 ± 1.3
SPE 12 U1-A	7634	1984.78 ± 0.43	3.1215 ± 0.005	0.0168 ± 0.00024	32.74 ± 0.25	132.5 ± 1.5	1.63 ± 0.01	1.59 ± 0.02	133.1 ± 1.6
SPE 12 U1-B	7415	791.688 ± 0.084	1.6515 ± 0.0039	0.01328 ± 0.00031	19.53 ± 0.22	132.3 ± 1.7	1.288 ± 0.01	1.23 ± 0.03	132.8 ± 1.7

[a] All ages are corrected for detrital Th assuming bulk Earth ^{232}Th/^{238}U weight ratio of 3.8 ± 1.9 for the detritus and ^{230}Th, ^{234}U and ^{238}U in secular equilibrium.

Table 4
^{36}Cl dating results of the six samples collected from SPE 5N, SPE 8, SPE 12 and SPE 14.

Sample ID	Sample mass (g)	Cl spike (mg)	Blank corr. (%)	^{35}Cl/^{37}Cl	^{36}Cl/^{35}Cl (10^{-14})	Natural Cl (μg/g)	^{36}Cl (10^5 atoms/g)	Unc. ^{36}Cl (%)	ICP-OES measurements of dissolved aliquot					^{36}Cl inheritance (10^5 atoms/g)[b]	^{36}Cl since overturning (10^4 atoms/g)	Unc. ^{36}Cl since overturning (%)	t_1: age since overturning (ka)
									CaO (%)	K_2O (%)	TiO_2 (%)	Fe_2O_3 (%)	MgO (%)				
SPE 5N Cl1	43.348	1.517	3.9	3.46	4.15 ± 0.49	346 ± 41	2.00 ± 0.33	16.5	53.2	0.020	0.000	0.001	0.076	12.8 ± 1.3	7.2 ± 3.5	49	2.9 ± 1.4
SPE 5N Cl2	43.505	1.548	3.6	3.42	3.94 ± 0.39	399 ± 53	2.17 ± 0.35	16.1	53.1	0.021	0.000	0.000	0.107	13.6 ± 1.8	8.1 ± 3.9	48	3.0 ± 1.4
SPE 8 Cl	43.814	1.505	3.9	3.42	3.75 ± 3.70	382 ± 50	1.97 ± 0.32	16.1	52.9	0.019	0.000	0.003	0.082	13.0 ± 1.2	6.7 ± 3.4	51	2.5 ± 1.3
SPE 12 Cl	39.826	1.616	1.4	3.55	7.69 ± 0.53	313 ± 30	3.55 ± 0.38	10.7	53.0	0.075	0.000	0.007	0.088	21.3 ± 2.0	14.2 ± 4.3	30	6.1 ± 1.8
SPE 14 Cl1	43.507	1.512	3.2	3.51	5.76 ± 0.63	292 ± 30	2.40 ± 0.35	14.6	53.1	0.017	0.000	0.002	0.084	17.4 ± 1.8	6.6 ± 3.9	60	2.9 ± 1.7
SPE 14 Cl2	40.585	1.868	0.4	3.48	1.94 ± 0.10	421 ± 45	11.9 ± 1.3	10.9	52.6	0.070	0.000	0.010	0.104	–	–	–	–
BL19	–	1.544	–	20.02	1.39 ± 0.37	–	–	–	–	–	–	–	–	–	–	–	–
BL24[a]	–	1.722	–	19.26	7.0 ± 1.3	–	–	–	–	–	–	–	–	–	–	–	–

[a] For samples SPE 12Cl and SPE 14 Cl2.
[b] The calculation of the ^{36}Cl inheritance for each boulder, since the emersion of the MIS 5.5 coral reef platform (~120 ka) is based on the ^{36}Cl concentration of sample SPE 14 Cl2 (bottom side of the boulder, $N_{bottom,t0[inh]}$) and a denudation rate of the platform amounting to 21 ± 5 mm/ka (see text for further explications).

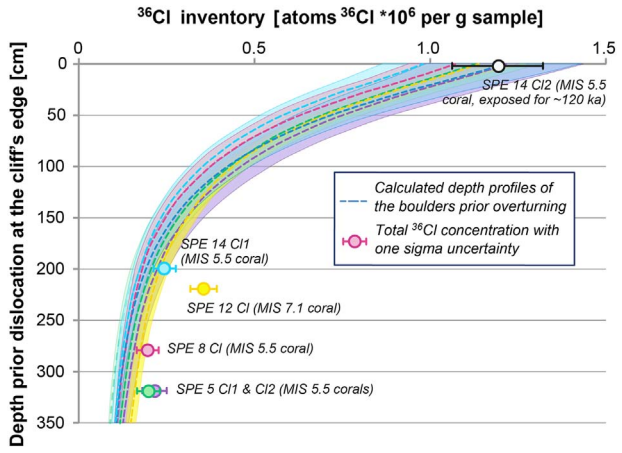

Fig. 7. ^{36}Cl concentrations of the six samples collected from four different boulders and calculation of depth profiles based on the thickness of each individual boulder (i.e. depth prior to dislocation). We calculated a denudation rate of 21 ± 5 mm/ka using the concentration of sample SPE 14 Cl2 (current bottom surface of the boulder).Note that the scaled production rate changes in each boulder (see Supplementary material 5), mostly as a result of variable densities and different concentrations of stable chlorine, which strongly influences the production by thermal neutrons.

($N_{top,t1}$), the capture of thermal neutrons represents the main production pathway at depths greater than ~20 cm in our coral samples. This is problematic because the magnitude and behaviour of the thermal neutron flux cannot be precisely reconstructed since it strongly depends on the hydrogen content of the environment (e.g. Phillips et al., 2001; Dunai, 2010; Dunai et al., 2014; Marrero et al., 2016). For instance, a hydrogen-rich cover multiplies the thermal neutron flux in the underlying rock by a factor of up to three (Dunai et al., 2014). Thus, any environmental moisture, such as episodic rainwater storage in rook pools, might have enhanced the thermal ^{36}Cl production rate. Since we calculated the ^{36}Cl ages assuming no hydrogen cover, the produced overturning ages should be considered as maximum age estimates.

Secondly, uncertainties related to the density determination of the dated material may significantly impact the calculation of inheritance and, thereby, the inferred exposure ages. However, density assessments used in this study for the dated boulders are those of Engel and May (2012), who precisely determined their bulk densities based on thorough examination of the variable coralline lithofacies. We therefore assume that these values are suitable to infer a reliable inherited component.

Thirdly, we used a constant denudation rate of 21 ± 5 mm/ka, integrated over the last 120 ka. This value is based on the ^{36}Cl concentration of SPE 14 Cl2 and the aerial exposure of the coral reef-platform since its emersion shortly after the MIS 5.5 (~120 ka). The latter is inferred from ^{230}Th/U ages of the LT (Obert et al., 2016 and age therein). Although the denudation rate most likely varied over time, this value is similar to the denudation rate of 10–20 mm/ka deduced for the LT of the ABC islands (Focke, 1978). We therefore assume that this integrated value can be used as a realistic proxy and we emphasize that uncertainties related to variations in the denudation rate are within the other uncertainties.

Finally, the last source of uncertainty is related to the extrapolation of the production rates to mid-Holocene timescales since the three primary calibration sites for ^{36}Cl have exposure ages ranging from 11.7 to 18.2 ka (Marrero et al., 2016).

A similar approach for dating such an overturning event was presented by Fujioka et al. (2014), who investigated fluvially transported boulders in the monsoonal tropics of Australia. In comparison to our study relying on ^{36}Cl concentrations, they used ^{10}Be and ^{26}Al concentrations (sandstone material) and benefited from this twofold information for each dated boulder on the one hand. On the other hand, they sampled much thinner boulders (i.e. thickness ranging between

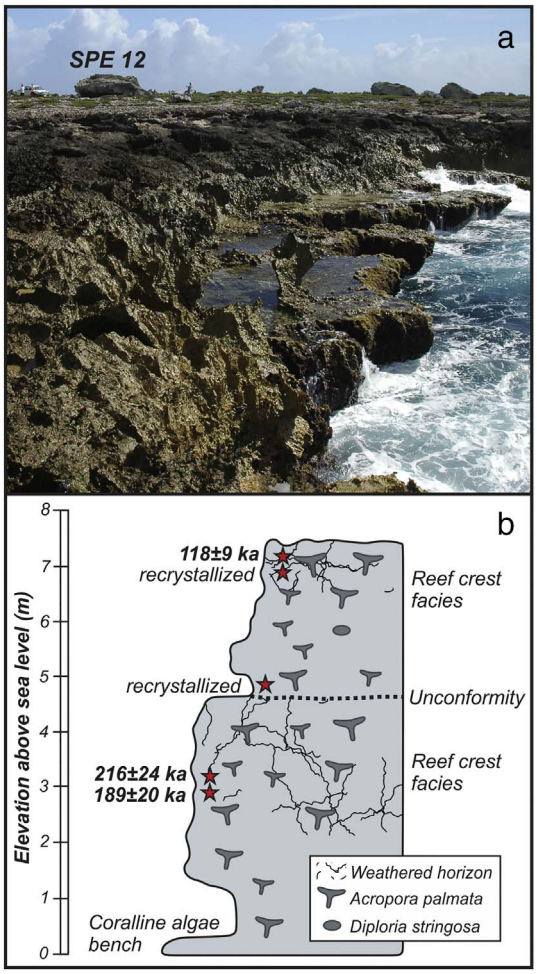

Fig. 8. a) Cliff's edge in the seaward prolongation of SPE 12, with hypothetical platform boundary between MIS 7 and MIS 5.5, possibly implying an older source area of boulder SPE 12 that would explain the ^{230}Th/U ages clustering between ~190 and ~211 ka (see Supplementary material 6). b) ESR dating revealed stacked coral-reef terraces (MIS 5.5 over MIS 7) at Curaçao, an island located ~50 km to the west of Bonaire (Leeward Antilles).
Modified from Schellmann et al. (2004).

0.5 and 0.9 m) than those presented here and thus had to face other complications, for instance related to inheritance. The robustness of their data inferred from six investigated boulders is difficult to assess since two of them could not be dated (i.e. steady-state profiles), whilst the remaining four yielded either Middle/Late Pleistocene ages or Holocene ages. Given the convergence of the nominal ^{36}Cl ages of three out of four dated boulders (SPE 5: 2.9-3.0 ka, SPE 8: 2.5 ka and SPE 14: 2.9 ka), we assume that the dating method based on cosmogenic nuclides measurements is more precise than originally expected.

At last, despite the fact that the 6.1 ± 1.8 ka age of boulder SPE 12 slightly overlaps the 1σ time span defined by other ^{36}Cl ages (Fig. 6), it could point to an older dislocation and transport event as well. However, the higher ^{36}Cl concentration of sample SPE 12 Cl might also be related to a greater inheritance. Indeed, supplementary ^{230}Th/U dating of material collected from the boulder SPE 12, though suffering from high uncertainties, range between ~190 and ~211 ka (sample SPE 12 U2-A, -B, -C stemming from a bulge inside a former rock pool, see Supplementary material 5). These ages potentially point to the MIS 7 and would imply that the source area at the cliff edge for the boulder SPE 12 (Fig. 8a), the southernmost investigated boulder at Spelonk (Fig. 1), might be older than the one of the three boulders located further north. ESR dating of coral-reef platforms on Curaçao, an island adjacent to Bonaire framed by a very similar staircase of uplifted interglacial reef terraces, show the local stacking of the MIS 5.5 terrace onto the MIS 7 terrace, which had formed under a lower sea level highstand (Fig. 8b) (Schellmann et al., 2004; Muhs et al., 2012) and support this hypothesis. If corals forming the boulder SPE 12 originate from the lower-lying MIS 7 terrace, they accordingly accumulated a higher inherited component as they underwent a much longer pre-exposition during two cold stages (MIS 6 and MIS 2) instead of only one. However, since no sample was collected at the current underside of this boulder, we are unable to correct the concentration of SPE 12 Cl for a possible higher inheritance. Given the large uncertainties that are involved, the question whether the age of 6.1 ± 1.8 ka points to an older transport event or not (higher inheritance) remains speculative.

5.3. Reliability of minimum ^{230}Th/U ages and their implications for tsunami history on Bonaire

The two ^{230}Th/U corrected ages obtained on the post-depositional flowstone (SPE 12 U1-A and U1-B) are in stratigraphic order: the older and younger layers (S2 and S3) yield ages of 1.59 ± 0.02 and 1.23 ± 0.03 ka, respectively. Note that the ^{230}Th/U corrected age obtained on the microbialite (1.23 ± 0.23 ka), though much less precise after correction for detrital Th, is in good agreement with the two previous ages. We thus state that secondary calcite flowstone, provided that the ^{232}Th content is low, constitutes the most appropriate sampling material for post-depositional ^{230}Th/U dating of transported boulders. If not present, subaerial Mg-calcite microbialites may represent a useful alternative, provided that age correction for detrital Th is systematically performed. XRD and XRF analyses are also highly recommended to investigate the mineralogical and inorganic element compositions of the microbialites, respectively (Fig. 5f–g). It is also worth noting the good concordance between ^{230}Th/U dating (minimum ages) and ^{36}Cl surface exposure dating (timing of transport). With the exception of boulder SPE 12 for which the probable higher inheritance cannot be quantified, the three ^{230}Th/U minimum ages are either slightly younger or partially overlap the exposure ages, within their 1σ confidence interval, of boulders SPE 5, 8 and 14 (Fig. 6).

Whilst our new age data do not contradict the observation that the coral reef did not regenerate during the last 3.1 ka along the eastern coast of Bonaire (Scheffers et al., 2006), they can also be compared with age data of Scheffers et al. (2014) obtained on supratidal coral ramparts and rubble ridges and with extreme wave events identified in the fine-grained sediment record (Fig. 9), i.e. around 3.6 ka (event I), 3.3 ka (II), post-2 ka (XII) and 0.5–1.3 ka (XVI) (Engel et al., 2012, 2013). Based on the distribution of ^{230}Th/U ages of coral rubble from Spelonk, Scheffers et al. (2014) assumed a deposition of the studied boulder field during extreme wave event II with a maximum age of 3.3 ka (Fig. 9). On the one hand, the ^{36}Cl age cluster, given its large uncertainties (see Section 5.2), spans extreme wave events I, II, XII and partially XVI, and thus cannot discriminate between them (Fig. 9). On the other hand, the corrected age obtained on the first post-depositional flowstone layer (sample SPE 12 U1-A) points to a minimum age of 1.6 ka for the transport of boulder SPE 12.

As for ^{230}Th/U minimum ages, the key question is whether a significant time-lag has occurred – or not – between boulder deposition and secondary calcite precipitation. It remains the main limitation of this dating method in this context. Unfortunately, there are so far few comparable observations documenting such phenomenon on supra-littoral boulders. However, secondary calcite precipitation was already reported in other contexts: for instance, incipient flowstone curtain, very similar to our flowstone occurrence on Bonaire, has been described by Sanders et al. (2010) at the underside of boulders of the Holocene Tschirgant rockslide (Austria). Based on the same dating method, Sanders et al. (2010) explicitly supported the hypothesis that calcite precipitation occurred immediately or shortly after the event. On Bonaire, the occurrence of a potentially wetter period enhancing carbonate dissolution during the 1–1.6 ka time period contradicts the

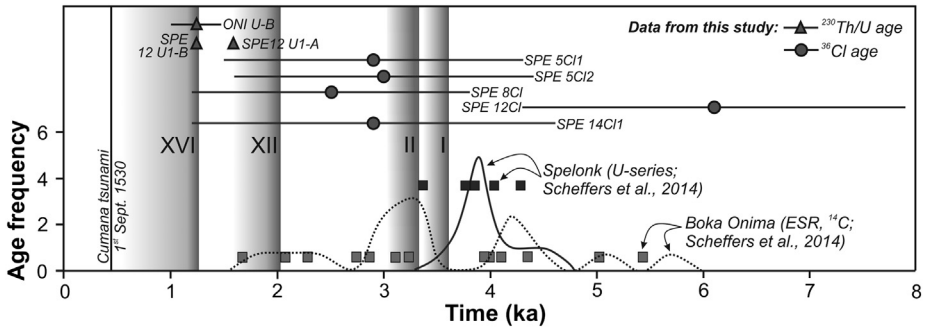

Fig. 9. Age/frequency diagram of inferred past high-energy wave events from sites lying at the eastern coast of Bonaire, modified from Scheffers et al. (2014). Gray shaded areas represent time periods for events based on the fine-grained sediment record (Engel et al., 2012). Whilst the imprecision related to the ^{36}Cl exposure ages hampers any correlation with a specific event, the minimum ^{230}Th/U age at Spelonk fairly well matches EWE XII, provided that precipitation of secondary flowstone occurred shortly after deposition.

main trend toward drier conditions since the mid-Holocene evidenced in the neighbouring Cariaco basin (Haug et al., 2001). Since the twofold carbonate dissolution/$CaCO_3$ precipitation process seems not primarily controlled by major climatic fluctuations on Bonaire, we may assume that flowstone development occurred within a short time span after the transport event too. Thus, our 1.59 ± 0.02 age would rather suggest a correlation with event XII (2.0–1.7 ka; Fig. 9), whose fine-grained deposits have been identified at Lagun, south of the Spelonk boulder field (Engel et al., 2010). Interestingly, the cluster of ^{230}Th/U minimum ages between 1.0 and 1.6 ka is obtained on boulders lying on the LT at Spelonk (flowstone) and Boka Onima (microbialite), both sites being > 10 km distant from each other (Fig. 1).

6. Conclusions

This study aimed to (i) compare three independent dating methods to constrain the timing of dislocation and transport of tsunami-induced reef-top boulders on Bonaire and (ii) discuss their potential and current limitations. The implementation of surface exposure dating via ^{36}Cl concentration measurements of corals, which represents a first attempt in this context, was motivated by the following arguments: (i) availability of > 2 m-thick boulders with field evidences of complete overturning during transport; (ii) good constraints of the boulders' source area, i.e. the reef platform edge, and timing of reef platform formation; and (iii) a good knowledge of the boulders' bulk densities. Although several factors, especially the high stable chlorine content in all samples, hamper the deduction of a precise timing for dislocation, transport and overturning of boulders, three of the four dated boulders at Spelonk cluster around 2.5-3.0 ka (nominal ages). This result thus suggests that surface exposure ages based on cosmogenic nuclides measurements might represent a useful and reliable dating tool in similar settings, provided that uncertainties inherent to this method (chemical composition and density of boulders, inheritance, denudation rates) can be minimized. Note also that our sampling approach developed for ^{36}Cl surface exposure dating is not restricted to tsunami-induced transport but could be likewise applied to storm-induced transport, as long as one single complete overturning of the boulder can be assessed.

By contrast, we showed that radiocarbon ages of boring bivalves, because of post-mortem carbonate dissolution, recrystallization and replacement (i.e. neomorphism), may dramatically overestimate the timing of dislocation. This method is thus considered as inappropriate in our setting; we therefore strongly recommend careful field examination and critical result interpretation before drawing any age inference of extreme wave events based on such data. Our data show that ^{230}Th/U dating of post-depositional flowstone is the most suitable method to yield minimum ages for boulder deposition. If not present, subaerial, Mg-calcite microbialites may represent a useful alternative, provided that age correction for detrital Th is systematically performed. Also, XRD and XRF analyses are recommended to investigate the mineralogical and inorganic element compositions of the microbialites, respectively.

Finally, based on the ^{230}Th/U age of the oldest flowstone layer, we could infer a minimum age of 1.6 ka for an extreme wave event at Spelonk, possibly pointing to a younger event (XII) than those suggested so far for the boulder field. Whilst potential post-depositional reworking of the coral material dated from ridges and rubbles (^{14}C, ESR, ^{230}Th/U; Scheffers et al., 2014) questions the reliability of this approach to infer a chronological framework for tsunami occurrence, careful sampling of suitable post-depositional features for ^{230}Th/U dating allows this issue to be disregarded. The same holds for ^{36}Cl surface exposure ages. Further research is however required to determine whether one or several event(s) occurred during the late Holocene at the Spelonk boulder field on Bonaire.

Acknowledgments

We kindly thank Prof. Juan C. Braga (Departamento de Estratigrafía y Paleontología, Universidad de Granada, Spain) and Dr. Shasta Marrero (School of Geosciences, University of Edinburgh) for the insightful discussions about microbialites and the muogenic ^{36}Cl production rate, respectively. We also thank Dr. Stephan Opitz (Institute of Geography, University of Cologne) for the XRD and XRF measurements of the microbialite sample and Rebecca Keulertz (Institute of Geology, University of Cologne) for assistance during sample preparation for ^{36}Cl surface exposure dating. Pertinent remarks provided by two anonymous reviewers significantly improved the quality of the manuscript. We are also indebted to the different funding sources, which allowed the achievement of this study: the Bernd Rendel Prize (*Deutsche Forschungsgemeinschaft* [*DFG*], EN 977/1-1), the Max Delbrück Prize (Zukunftskonzept Universität zu Köln, DFG ZUK 81/1), the ABC/J Research Award and the Dr. Hohmann Funding (*Gesellschaft für Erdkunde zu Köln e. V.*).

Appendix A. Supplementary data

Supplementary data and information to this article can be found online at http://dx.doi.org/10.1016/j.margeo.2017.03.007.

References

Balco, G., 2011. Contributions and unrealized potential contributions of cosmogenic-nuclide exposure dating to glacier chronology, 1990–2010. Quat. Sci. Rev. 30, 3–27.
Barbano, M.S., Pirrotta, C., Gerardi, F., 2010. Large boulders along the south-eastern Ionian coast of Sicily: storm or tsunami deposits? Mar. Geol. 275, 140–154.
Bard, E., Hamelin, B., Fairbanks, R.G., 1990. U-Th ages obtained by mass spectrometry in corals from Barbados: sea level during the past 130,000 years. Nature 346, 456–458.
Biolchi, S., Furlani, S., Antonioli, F., Baldassini, N., Deguara, J.C., Devoto, S., Di Stefano, A., Evans, J., Gambin, T., Gauci, R., Mastronuzzi, G., Monaco, C., Scicchitano, G.,

2016. Boulder accumulations related to extreme wave events on the eastern coast of Malta. Nat. Hazards Earth Syst. Sci. 16, 737–756.
Blair, T.C., McPherson, J.G., 1999. Grain-size and textural classification of coarse sedimentary particles. J. Sediment. Res. 69, 6–19.
Braucher, R., Merchel, S., Borgomano, J., Bourlès, D.L., 2011. Production of cosmogenic radionuclides at great depth: a multi element approach. Earth Planet. Sci. Lett. 309, 1–9.
Brill, D., Klasen, N., Brückner, H., Jankaew, K., Kelletat, D., Scheffers, A., Scheffers, S., 2012. Local inundation distances and regional tsunami recurrence in the Indian Ocean inferred from luminescence dating of sandy deposits in Thailand. Nat. Hazards Earth Syst. Sci. 12, 2177–2192.
Brocas, W.M., Felis, T., Obert, J.C., Gierz, P., Lohmann, G., Scholz, D., Kölling, M., Scheffers, S.R., 2016. Last interglacial temperature seasonality reconstructed from tropical Atlantic corals. Earth Planet. Sci. Lett. 449, 418–429.
Buckley, M.L., Wei, Y., Jaffe, B.E., Watt, S.G., 2012. Inverse modeling of velocities and inferred cause of overwash that emplaced inland fields of boulders at Anegada, British Virgin Islands. Nat. Hazards 63, 133–149.
Cheng, H., Edwards, R., Hoff, J., Gallup, C., Richards, D., Asmerom, Y., 2000. The half-lives of uranium-234 and thorium-230. Chem. Geol. 169, 17–33.
Cisternas, M., Atwater, B.F., Torrejon, F., Sawai, Y., Machuca, G., Lagos, M., Eipert, A., Youlton, C., Salgado, I., Kamataki, T., Shishikura, M., Rajendran, C.P., Malik, J.K., Rizal, Y., Husni, M., 2005. Predecessors of the giant 1960 Chile earthquake. Nature 437, 404–407.
De Buisonjé, P.H., 1974. Neogene and Quaternary geology of Aruba, Curaçao and Bonaire (Netherlands Antilles). (Ph.D. Thesis) Rijksuniversiteit Utrecht.
Desilets, D., Zreda, M., Almasi, P.F., Elmore, D., 2006. Determination of cosmogenic ^{36}Cl in rocks by isotope dilution: innovations, validation and error propagation. Chem. Geol. 233, 185–195.
Douka, K., Hedges, R.E.M., Higham, T.F.G., 2010. Improved AMS 14C dating of shell carbonates using high-precision X-ray diffraction and a novel density separation protocol (CarDS). Radiocarbon 52, 735–751.
Douville, E., Sallé, E., Frank, N., Eisele, M., Pons-Branchu, E., Ayrault, S., 2010. Rapid and accurate U–Th dating of ancient carbonates using inductively coupled plasma-quadrupole mass spectrometry. Chem. Geol. 272, 1–11.
Dunai, T.J., 2010. Cosmogenic Nuclides, Principles, Concepts and Applications in the Earth Surface Sciences. Cambridge University Press, UK.
Dunai, T.J., Binnie, S.A., Hein, A.S., Paling, S.M., 2014. The effects of a hydrogen-rich ground cover on cosmogenic thermal neutrons: implications for exposure dating. Quat. Geochronol. 22, 183–191.
Engel, M., May, S.M., 2012. Bonaire's boulder fields revisited: evidence for Holocene tsunami impact on the Leeward Antilles. Quat. Sci. Rev. 54, 126–141.
Engel, M., Bruckner, H., Wennrich, V., Scheffers, A., Kelletat, D., Vött, A., Schäbitz, F., Daut, G., Willerhäuser, T., May, S.M., 2010. Coastal stratigraphies of eastern Bonaire (Netherlands Antilles): New insights into the palaeo-tsunami history of the southern Caribbean. Sed. Geol. 231, 14–30.
Engel, M., Brückner, H., Messenzehl, K., Frenzel, P., May, S.M., Scheffers, A., Scheffers, S., Wennrich, V., Kelletat, D., 2012. Shoreline changes and high-energy wave impacts at the leeward coast of Bonaire (Netherlands Antilles). Earth Planets Space 64, 905–921.
Engel, M., Brückner, H., Fürstenberg, S., Frenzel, P., Konopczak, A.M., Scheffers, A., Kelletat, D., May, S.M., Schäbitz, F., Daut, G., 2013. A prehistoric tsunami induced long-lasting ecosystem changes on a semi-arid tropical island – the case of Boka Bartol (Bonaire, Leeward Antilles). Naturwissenschaften 100, 51–67.
Engel, M., Oetjen, J., May, S.M., Brückner, H., 2016. Tsunami deposits of the Caribbean - towards an improved coastal hazard assessment. Earth Sci. Rev. 163, 260–296.
Etienne, S., Buckley, M., Paris, R., Nandasena, A.K., Clark, K., Strotz, L., Chagué-Goff, C., Goff, J., Richmond, B., 2011. The use of boulders for characterising past tsunamis: lessons from the 2004 Indian Ocean and 2009 South Pacific tsunamis. Earth Sci. Rev. 107, 76–90.
Felis, T., Giry, C., Scholz, D., Lohmann, G., Pfeiffer, M., Pätzold, J., Kölling, M., Scheffers, S.R., 2015. Tropical Atlantic temperature seasonality at the end of the last interglacial. Nat. Commun. 6, 6159.
Focke, J.W., 1978. Limestone cliff morphology on Curaçao (Netherlands Antilles), with special attention to the origin of notches and vermetid/coralline algal surf benches ("corniches", "trottoirs"). Z. Geomorph. 22, 329–349.
Frankel, K.L., Brantley, K.S., Dolan, J.F., Finkel, R.C., Klinger, R.E., Knott, J.R., Machette, M.N., Owen, L.A., Phillips, F.M., Slate, J.L., Wernicke, B.P., 2007. Cosmogenic ^{10}Be and ^{36}Cl geochronology of offset alluvial fans along the northern Death Valley fault zone: implications for transient strain in the eastern California shear zone. J. Geophys. Res. Solid Earth 112, B06407.
Frohlich, C., Hornbach, M.J., Taylor, F.W., Shen, C.C., Moala, A., Morton, A.E., Kruger, J., 2009. Huge erratic boulders in Tonga deposited by a prehistoric tsunami. Geology 37, 131–134.
Fujioka, T., Fink, D., Nanson, G., Mifsud, C., Wende, R., 2014. Flood-flipped boulders: in-situ cosmogenic nuclide modeling of flood deposits in the monsoon tropics of Australia. Geology 43, 43–46.
Gosse, J.C., Phillips, F.M., 2001. Terrestrial in situ cosmogenic nuclides: theory and application. Quat. Sci. Rev. 20, 1475–1560.
Goto, K., Okada, K., Imamura, F., 2010. Numerical analysis of boulder transport by the 2004 Indian Ocean tsunami at Pakarang Cape, Thailand. Mar. Geol. 268, 97–105.
Haug, G.H., Hughen, K.A., Sigman, D.M., Peterson, L.C., Röhl, U., 2001. Southward migration of the intertropical convergence zone through the Holocene. Science 293, 1304–1308.
Jackson, T.A., Robinson, E., 1994. The Netherlands and Venezuelan Antilles. In: Donovan, S.K., Jackson, T.A. (Eds.), Caribbean Geology: An Introduction. University of the West Indies Press, Kingston, pp. 249–263.
Jones, B., Hunter, I.G., 1992. Very large boulders on the coast of Grand Cayman: the effects of Giant waves on rocky coastlines. J. Coast. Res. 8, 763–774.
Khan, S., Robinson, E., Rowe, D.-A., Coutou, R., 2010. Size and mass of shoreline boulders moved and emplaced by recent hurricanes, Jamaica. Z. Geomorphol. 54 (Suppl. Band 3), 281–299.
Kim, K.H., Lee, D.-J., 1999. Distribution and depositional environments of corraline lithofacies in uplifted Pleistocene coral reefs of Bonaire, Netherlands Antilles. J. Paleontol. Soc. Korea 15 (155–133).
Lal, D., Gallup, C.D., Somayajulu, B.L.K., Vacher, L., Caffee, M.W., Jull, A.J.T., Finkel, R.C., Speed, R.C., Winter, A., 2005. Records of cosmogenic radionuclides ^{10}Be, ^{26}Al and ^{36}Cl in corals: first studies on coral erosion rates and potential of dating very old corals. Geochim. Cosmochim. Acta 69, 5717–5728.
Léveillé, R.J., Fyfe, W.S., Longstaffe, F.J., 2000. Geomicrobiology of carbonate–silicate microbialites from Hawaiian basaltic sea caves. Chem. Geol. 169, 339–355.
Lorang, M.S., 2011. A wave-competence approach to distinguish between boulder and megaclast deposits due to storm waves versus tsunamis. Mar. Geol. 283, 90–97.
Marrero, S.M., Phillips, F.M., Caffee, M.W., Gosse, J.C., 2016. CRONUS-Earth cosmogenic ^{36}Cl calibration. Quat. Geochronol. 31, 199–219.
May, S.M., Engel, M., Brill, D., Cuadra, C., Lagmay, A.M.F., Santiago, J., Suarez, J.K., Reyes, M., Brückner, H., 2015a. Block and boulder transport in Eastern Samar Philippines during Supertyphoon Haiyan. Earth Surf. Dyn. 3, 543–558.
May, S.M., Brill, D., Engel, M., Scheffers, A., Opitz, S., Wennrich, V., Squire, P., Kelletat, D., Brückner, H., 2015b. Traces of historical tropical cyclones and tsunamis in the Ashburton Delta (NW Australia). Sedimentology 62, 1546–1572.
Miller, S., Rowe, D.-A., Brown, L., Mandal, A., 2014. Wave-emplaced boulders: implications for development of "prime real estate" seafront, North Coast Jamaica. B. Eng. Geol. Environ. 73, 109–122.
Morton, R.A., Richmond, B.M., Jaffe, B.E., Gelfenbaum, G., 2006. Reconnaissance investigation of Caribbean extreme wave deposits – preliminary observations, interpretations, and research directions. In: USGS Open-File Report, 2006–1293, .
Morton, R.A., Richmond, B.M., Jaffe, B.E., Gelfenbaum, G., 2008. Coarse-clast ridge complexes of the Caribbean: a preliminary basis for distinguishing tsunami and storm-wave origins. J. Sediment. Res. 78, 624–637.
Muhs, D.R., Pandolfi, J.M., Simmons, K.R., Schumann, R.R., 2012. Sea-level history of past interglacial periods from uranium-series dating of corals, Curaçao, Leeward Antilles islands. Quat. Res. 78, 157–169.
Obert, J.C., Scholz, D., Felis, T., Brocas, W.M., Jochum, K.P., Andreae, M.O., 2016. ^{230}Th/U dating of Last Interglacial brain corals from Bonaire (southern Caribbean) using bulk and theca wall material. Geochim. Cosmochim. Acta 178, 20–40.
Phillips, F.M., Zreda, M.G., Smith, S.S., Elmore, D., Kubik, P.W., Sharma, P., 1990. Cosmogenic chlorine-36 chronology for glacial deposits at bloody canyon, Eastern Sierra Nevada. Science 248, 1529–1532.
Phillips, F.M., Stone, W.D., Fabryka-Martin, J.T., 2001. An improved approach to calculating low-energy cosmic-ray neutron fluxes near the land/atmosphere interface. Chem. Geol. 175, 689–701.
Pijpers, P.J., 1933. Geology and Paleontology of Bonaire (D.W.I.). Geographische en Geologische Mededeelingen, Physiographisch-Geologische Reeks 8.
Prager, C., Ivy-Ochs, S., Ostermann, M., Synal, H.-A., Patzelt, G., 2009. Geology and radiometric ^{14}C-, ^{36}Cl- and Th-/U-dating of the Fernpass rockslide (Tyrol, Austria). Geomorphology 103, 93–103.
Prendergast, A., Cupper, M.L., Jankaew, K., Sawai, Y., 2012. Indian Ocean tsunami recurrence from optical dating of tsunami sand sheets in Thailand. Mar. Geol. 295–298, 20–27.
Reimer, P.J., Bard, E., Bayliss, A., Beck, J.W., Blackwell, P.G., Ramsey, C.B., Buck, C.E., Cheng, H., Edwards, R.L., Friedrich, M., Grootes, P.M., Guilderson, T.P., Haflidason, H., Hajdas, I., Hatté, C., Heaton, T.J., Hoffmann, D.L., Hogg, A.G., Hughen, K.A., Kaiser, K.F., Kromer, B., Manning, S.W., Niu, M., Reimer, R.W., Richards, D.A., Scott, E.M., Southon, J.R., Staff, R.A., Turney, C.S.M., van der Plicht, J., 2013. IntCal13 and Marine13 radiocarbon age calibration curves 0–50,000 years cal BP. Radiocarbon 55, 1869–1887.
Saint Martin, J.-P., Saint Martin, S., 2015. Discovery of calcareous microbialites in coastal ponds of western Sardinia (Italy). Geo-Eco-Marina 21, 35–53.
Sanders, D., Ostermann, M., Brandner, R., Prager, C., 2010. Meteoric lithification of catastrophic rockslide deposits: diagenesis and significance. Sediment. Geol. 223, 150–161.
Sato, T., Nakamura, N., Goto, K., Kumagai, Y., Nagahama, H., Minoura, K., 2014. Paleomagnetism reveals the emplacement age of tsunamigenic coral boulders on Ishigaki Island, Japan. Geology 42, 603–606.
Scheffers, A., 2002. Paleotsunami in the Caribbean: field evidences and datings from Aruba, Curaçao and Bonaire. In: Essener Geographische Arbeiten, pp. 33.
Scheffers, A., 2004. Tsunami imprints on the Leeward Netherlands Antilles (Aruba, Curaçao, Bonaire) and their relation to other coastal problems. Quat. Int. 120, 163–172.
Scheffers, A., 2005. Coastal response to extreme wave events – hurricanes and tsunamis on Bonaire. In: Essener Geographische Arbeiten, pp. 37.
Scheffers, A., Scheffers, S., 2006. Documentation of the impact of Hurricane Ivan on the coastline of Bonaire (Netherlands Antilles). J. Coast. Res. 22, 1437–1450.
Scheffers, S., Scheffers, A., Radtke, U., Kelletat, D., Straben, K., Bak, R., 2006. Tsunamis trigger long-lasting phase-shift in a coral reef ecosystem. Z. Geomorphol. Suppl. 146, 59–79.
Scheffers, A., Scheffers, S., Kelletat, D., Browne, T., 2009. Wave-emplaced coarse debris and megaclasts in Ireland and Scotland: boulder transport in a high-energy littoral environment. J. Geol. 117, 553–573.
Scheffers, A.M., Engel, M., May, S.M., Scheffers, S.R., Joannes-Boyau, R., Hänssler, E., Kennedy, K., Kelletat, D., Brückner, H., Vött, A., Schellmann, G., Schäbitz, F., Radtke, U., Sommer, B., Willershäuser, T., Felis, T., 2014. Potential and limits of combining studies of coarse- and fine-grained sediments for the coastal event history of a

Caribbean carbonate environment. In: Martini, I.P. (Ed.), Sedimentary Coastal Zones From High to Low Latitudes; Similarities and Differences. Geol. Soc. London Spec. Pub, vol. 388. pp. 503–531.

Schellmann, G., Radtke, U., Scheffers, A., Whelan, F., Kelletat, D., 2004. ESR dating of coral reef terraces on Curaçao (Netherlands Antilles) with estimates of Younger Pleistocene sea level elevations. J. Coast. Res. 20, 947–957.

Schimmelpfennig, I., Benedetti, L., Finkel, R., Pik, R., Blard, P.-H., Bourlès, D., Burnard, P., Williams, A., 2009. Sources of in-situ ^{36}Cl in basaltic rocks. Implications for calibration of production rates. Quat. Geochronol. 4, 441–461.

Schmidt, S., Hetzel, R., Kuhlmann, J., Mingorance, F., Ramos, V.A., 2011. A note of caution on the use of boulders for exposure dating of depositional surfaces. Earth Planet. Sci. Lett. 302, 60–70.

Scicchitano, G., Monaco, C., Tortorici, L., 2007. Large boulder deposits by tsunami waves along the Ionian coast of south-eastern Sicily (Italy). Mar. Geol. 238, 75–91.

Sharma, P., Kubik, P.W., Fehn, U., Gove, G.H., Nishiizumi, K., Elmore, D., 1990. Development of ^{36}Cl standards for AMS. Nucl. Inst. Methods Phys. Res. A B52, 410–415.

Spiske, M., Böröcz, Z., Bahlburg, H., 2008. The role of porosity in discriminating between tsunami and hurricane emplacement of boulders – a case study from the Lesser Antilles, southern Caribbean. Earth Planet. Sci. Lett. 268, 384–396.

Stone, J.O., 2000. Air pressure and cosmogenic isotope production. J. Geophys. Res. 105, 23753–23759.

Stone, J.O., Allan, G.L., Fifield, L.K., Cresswell, R.G., 1996. Cosmogenic chlorine-36 from calcium spallation. Geochim. Cosmochim. Acta 60, 679–692.

Terry, J.P., Etienne, S., 2014. Potential for timing high-energy marine inundation events in the recent geological past through age-dating of reef boulders in Fiji. Geosci. Lett. 1, 1–14.

Terry, J.P., Lau, A.Y.A., Etienne, S., 2013. Reef-platform Coral Boulders – Evidence for High-energy Marine Inundation Events on Tropical Coastlines. Springer, New York.

Watt, S.G., Jaffe, B.E., Morton, R.A., Richmond, B.M., Gelfenbaum, G., 2010. Description of extreme-wave deposits on the northern coast of Bonaire, Netherlands Antilles. In: USGS Open-file Report 2010–1180, .

Westermann, J.H., Zonneveld, J.I.S., 1956. Photo-geological Observations and Land Capability & Land Use Survey of the Island of Bonaire (Netherlands Antilles). Koninklijk Institut voor de Tropen, Amsterdam.